J Mater Sci (2011) 46:2662–2671
DOI 10.1007/s10853-010-5122-z

Microstructure evolution and hardness variation during annealing of equal channel angular pressed ultra-fine grained nickel subjected to 12 passes

K. Sitarama Raju · M. Ghanashyam Krishna · K. A. Padmanabhan · V. Subramanya Sarma · N. P. Gurao · G. Wilde

Received: 20 August 2010 / Accepted: 27 November 2010 / Published online: 16 December 2010

Abstract The microstructure, thermal stability and hardness of ultra-fine grained (UFG) Ni produced by 12 passes of equal channel angular pressing (ECAP) through the route Bc were studied. Comparing the microstructure and hardness of the as-ECAPed samples with the published data on UFG Ni obtained after 8 passes of ECAP through the route Bc reveals a smaller average grain size (230 nm in the present case compared with 270 nm in 8-pass Ni), significantly lower dislocation density (1.08×10^{14} m^{-2} compared with 9×10^{14} m^{-2} in 8-pass Ni) and lower hardness (2 GPa compared with 2.45 GPa for 8-pass Ni). Study of the thermal stability of the 12-pass UFG Ni revealed that recovery is dominant in the temperature range 150–250°C and recrystallisation occurred at temperatures >250 °C. The UFG microstructure is relatively stable up to about 400 °C. Due to the lower dislocation density and consequently a lower stored energy, the recrystallisation of 12-pass ECAP Ni occurred at a higher temperature (~250 °C) compared with the 8-pass Ni (~200 °C). In the 12-pass Nickel, hardness variation shows that its dependence on grain size is inversely linear rather than the common grain size$^{-0.5}$ dependence.

K. Sitarama Raju (✉) · M. Ghanashyam Krishna · K. A. Padmanabhan
School of Physics and Centre for Nanotechnology, University of Hyderabad, Hyderabad 500 046, India
e-mail: srk@deakin.edu.au

K. A. Padmanabhan
School of Engineering Sciences & Technology, University of Hyderabad, Hyderabad 500 046, India

K. A. Padmanabhan · G. Wilde
Institute of Materials Physics, University of Muenster, Wilhelm-Klemm-Strasse 10, 48149 Muenster, Germany

V. Subramanya Sarma
Department of Metallurgical and Materials Engineering, Indian Institute of Technology Madras, Chennai 600 036, India

N. P. Gurao
Department of Materials Engineering, Indian Institute of Science, Bangalore 560 012, India

Introduction

Bulk ultra-fine grained (UFG) (range ~100 nm–1 μm) and nanostructured (grain size <100 nm) materials produced using severe plastic deformation (SPD) techniques exhibit unique physical and mechanical properties or properties which differ vastly from those of their coarser variants. Such SPD-processed materials are of interest also because they are relatively free of residual porosity and contamination [1, 2]. Decreasing the grain size towards a lower limit [3] increases the strength broadly in accordance with the Hall–Petch (H–P) relationship- i.e., the yield stress, σ_y, is proportional to the inverse of the square root of the average grain size, d. Cryo-rolling [4], accumulative roll bonding [5, 6], equal channel angular pressing [1, 2, 7], high pressure torsion [1, 8] etc., and combinations thereof, have been shown to produce grain sizes down to 100 nm and below and there is a significant improvement in the mechanical properties, particularly the strength. The stacking fault energy (SFE), initial grain size prior to deformation (there is also a school of thought that the effect of this variable is insignificant), purity of metal, strain and the processing technique (which defines the state of stress applied) all determine the final grain size. Among the different SPD techniques, equal channel angular pressing (ECAP) is capable of producing relatively large billets [9]. In contrast, repeated cold rolling and folding has given rise

to the smallest grain sizes reported so far (less than 20 nm) [10].

Pure nickel (of medium SFE), when subjected to ECAP, resulted in a relatively homogeneous microstructure after 8 passes, with an average grain size of ~0.27–0.30 μm [11, 12]. Further grain refinement down to ~0.23 μm was possible by increasing the number of passes to 12 [13]. But, the microstructure after 12 passes was inhomogeneous [13]. To understand the stability of the ultra-fine grain size, a systematic study of the deformed and the annealed microstructures, along with the corresponding textures, is essential. Texture and grain growth kinetics in 8-pass nickel have been investigated in several studies [11, 14–19]. They revealed that the UFGs are relatively stable up to 200 °C. Grain growth is present beyond that temperature. While the grain size could be further refined by increasing the number of passes e.g., from 8 to 12 [13], the effects of these smaller grain sizes on the mechanical properties of the material are yet to be studied systematically.

In this study, the change in the average grain size of 12-pass ECAP nickel as a function of annealing temperature and time was investigated. The microstructures that developed after recovery and recrystallization processes were examined using electron back-scattering diffraction (EBSD) and atomic force microscopy (AFM). The changes in grain boundary character during the recovery of the cold worked ECAP structure were also studied. Changes in grain orientation spread (GOS) and grain average misorientation (GAM), which are measures of the long-range and the short-range intra-granular misorientations, were correlated with the changes in the grain size and hardness. The relevance (or otherwise) of the Hall–Petch relationship for this UFG material was checked and the present findings were also compared with the earlier results. Grain size evolution in nanostructured and ultra-fine grained Ni produced through other techniques e.g., electrodeposition, was not a concern of this investigation.

Experimental

A commercial high purity nickel cylinder of 12.7 mm diameter (purity of 99.98%) with an initial average grain size of ~110 μm was used. This material was obtained from the company Chempur and was sold in the "annealed" condition. No further information was supplied. But, the shape of the supplied material clearly suggests that it was deformed prior to annealing. This inference was reinforced by the observation of annealing twins in the microstructure of the as-received material. The Ni billet was pressed 12 times through a 90° ECAP die to introduce a strain of ~12 using the route B_C. After 12 passes some degree of inhomogeneity in grain size was observed [13]. The recrystallisation temperature was determined using a differential scanning calorimeter (DSC) supplied by TA Instruments. From the center of the ECAPed billet small discs of 0.5 mm thickness were cut perpendicular to the direction of extrusion using electric discharge machining. The grain size, its distribution, grain boundary statistics and the misorientations were determined using an EBSD set-up attached to a FEI SIRION Field Emission Gun (FEG) SEM operating at 20 kV. The results were analysed using TexSem Laboratories orientation imaging microscopy (OIM) software version 5.1. The images were cleaned using "grain confidence index (CI) standardization" and "neighbouring CI correlation" to remove the bad data points. A grain was defined as having a misorientation > 5, a minimum CI value of 0.1 and a minimum of 3 pixels. The deformed and recrystallised microstructures were imaged using Atomic Force Microscopy (AFM) (model SPA400 scanning probe microscope supplied by SII Ind. Japan). AFM images were processed using SPIWIN analysis software. Intermittent-contact Atomic Force Microscopy (IC-AFM) and EBSD were used to characterise the microstructures of the deformed and the annealed samples. As it is easier to prepare samples for AFM compared with TEM, in principle, the former technique could be very useful for the characterization of deformed and recovered microstructures. The samples for AFM and EBSD studies were ground on SiC abrasive papers down to a mesh size of 4,000, followed by polishing with diamond paste and with colloidal silica for at least 1 h. The samples were then electro-polished using a mixture of 78 ml perchloric acid, 90 ml distilled water, 730 ml ethanol and 100 ml butyl cellosolve. Vickers micro-hardness measurements were made using a Shimadzu micro-hardness tester with a load of 50 g for 45 s.

Experimental results

Differential scanning calorimetry

Figure 1 displays a DSC plot for the 12-pass nickel at heating rates in the range of 10–50 K min^{-1}. There is a broad exothermic peak with the onset and the peak (maximum) temperatures being at ~355 °C and ~370 °C respectively at a heating rate of 50 K min^{-1} and this range becomes narrower with decreasing heating rate. The peak is due to the stored energy, which is released during the recrystallisation of the deformed grains and subsequent grain growth. The authors believe that an additional contribution came from the ferromagnetic to paramagnetic transition in Ni which occurs at ~360 °C [14] and due to a positive change in the heat capacity in the transformation region this transition appears endothermic in character

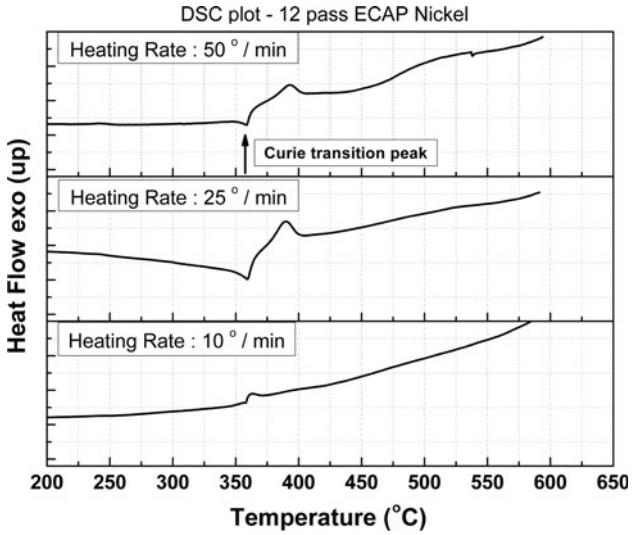

Fig. 1 DSC scan of ECAP Nickel from room temperature to 650 °C

(Fig. 1). Therefore, the net signature recorded in the DSC plot is the sum of these two opposing effects. Though the heating rate employed in the DSC experiment strongly influenced the position of the exothermic peak (caused by a release of the stored energy of deformation), the position of the endothermic peak (attributed to the Curie transition) is unchanged (Fig. 1). As a result, in the DSC scan performed at 10 K/min, the area under the exothermic peak is very small because of the overlapping endothermic Curie transition peak and the exothermic recrystallisation peak. This is consistent with the classification of Ehrenfest [15] that the Curie transition is a second order transformation and that it does not involve nucleation and growth and consequently is heating rate-independent. In contrast, recrystallisation, which occurs by nucleation and growth, is strongly dependent on the heating rate and this statement is consistent with this results.

Microscopic investigations

Atomic force microscopy—phase imaging

The microstructure of the 12-pass ECAP Ni was reported to be inhomogeneous with both elongated and equiaxed grains [13]. This is confirmed by the IC-AFM (also known as dynamic force microscopy (DFM)) phase contrast image shown in Fig. 2a.[1] The change in contrast in the phase image is due to a change in the phase of the vibrating tip from its reference value. This phase change is more evident near the boundaries i.e., near the distorted lattice, and minimum (or ~ 0) near strain-free areas. The colour coding on the scale bar extends from dark through bright in which the dark shaded areas represent the regions of negligible phase shift (less distortion) and bright shaded areas represent regions of greater phase shift (heavily distorted). The grain boundaries can be located by tracking the changes in the phase image. The IC-AFM images of the ECAPed and annealed samples (at 250 °C for 1 and 6 h) are shown in Fig. 2b and c, respectively. The phase profiles (Fig. 2d) plotted across the lines drawn in Fig. 2a–c, show the changes in phase in which the valleys in the plot are indicative of the presence of grain boundaries (marked GB in Fig. 2a–c). The region between two valleys could be considered as a grain and the small changes in phase between two valleys are due to the small lattice distortions within the grains. It can be seen that the overall phase change is more after 12 passes of ECAP and it is reduced following annealing at 250 °C for 1 and 6 h. The average grain size after 12 passes of ECAP obtained from AFM imaging is ~174 nm. After annealing at 250 °C for 1 and 6 h, the grain size increased to ~230 and ~340 nm, respectively. The above results show that the IC-AFM technique, due to its high resolution, could be used to study some details of the microstructure of bulk UFG/nanomaterials, which is not possible using other techniques (It will be useful to be more specific about this last point, by giving details).

Electron back scattering diffraction imaging

To obtain quantitative information on the grain boundary character, EBSD investigations were carried out on the as-ECAPed and annealed samples. Figure 3 shows the EBSD (unique grain colour) images of the as-received ECAP Ni (Fig. 3a) and samples annealed for 1 h at 250 °C (Fig. 3b), 300 °C (Fig. 3c) and 400 °C (Fig. 3d). Figure 3e shows the variation of equivalent circle diameter (ECD) grain size as a function of annealing temperature. Grain sizes were estimated by considering twin boundaries as grain boundaries (wt—with twins) as well as by not considering twin boundaries (wot—without twins). As to be expected, the grain size determined by considering twins is less than that "without twins" after annealing at temperatures $\geq$ 350 °C. Interestingly, the wt-grain size after annealing at 400 °C is less than that obtained after annealing at 350 °C. This is attributed to the formation of fine twin ledges or closed twins (Fig. 3d) due to grain boundary migration during recrystallisation/grain growth (see also the Discussion section).

To study the recovery process in detail, samples annealed at 150 °C for 1 h through 6 h were evaluated by EBSD. When the ECAP sample was annealed at 150 °C for

[1] A conventional AFM image (image of topography) is obtained by recording the changes in the vibrational amplitude (deflection) during scanning. In contrast, a phase image is obtained by monitoring the phase change between the input signal that drives the cantilever and the output signal.

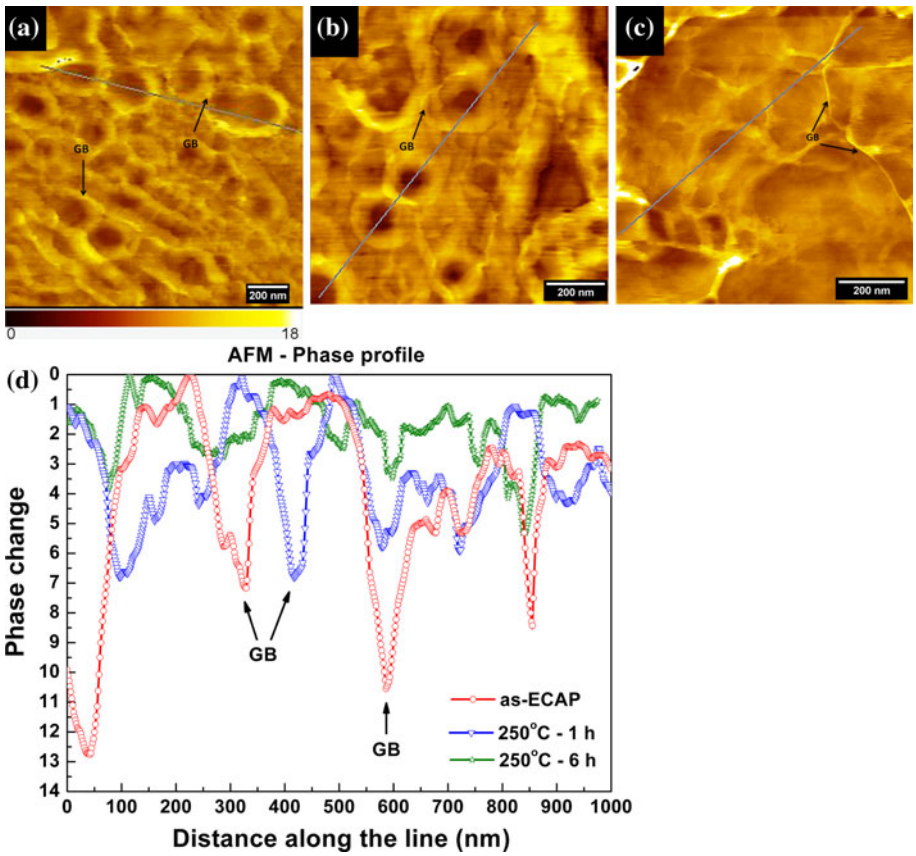

Fig. 2 Intermittent-contact Atomic Force Microscope (IC-AFM) phase image of the as-ECAPed material (**a**), after annealing at 250 °C for 1 h (**b**), 6 h (**c**) and the plot of phase shift profile across the *line* drawn in the respective images (**d**). Grain boundaries are marked as 'GB'

1 h, the area fraction of smaller grains (<1 μm) had decreased to ~39% from ~53% and that of larger grains (~3–5 μm) had increased to 17% from ~5%. The average grain size after annealing at 150 °C for 1 h was ~0.40 μm compared with a grain size of ~0.23 μm in the as ECAPed condition.

Evaluation of boundary fractions shows that the fraction of CSL Σ1 boundaries had increased after annealing at 150 °C for 1 h (compared with the as-ECAPed material) but it decreased after annealing at 3 and 6 h (Fig. 4a). The LAB fraction after 1, 3 and 6 h annealing was 37 ± 2, 20.5 ± 1 and 22.8 ± 1 (all in percentages), respectively. The increase from 3 to 6 h is not much significant and is within the experimental error. An increase in the twin boundary (Σ3 type) fraction was observed after 6 h annealing. This increase signifies the onset/presence of recrystallisation [16].

Grain orientation spread (GOS) and grain average misorientation (GAM) are often used to quantify the local misorientation distributions obtained from the EBSD scans. (GOS is defined as the average deviation in orientation between any given measurement in the grain and the average orientation of the grain. GAM is defined as the average misorientation between all the neighbouring pairs of measurements in a grain.) The above two parameters, by definition, are the measures of the long-range and the short-range misorientations within a grain. Figure 4b shows the variation of GOS and GAM as a function of annealing temperature. For the recrystallised grains, the GOS and GAM values are typically less than 2 [17]. As GOS increases with grain size, a more stringent criterion with GOS ≤1 can be used to differentiate the recrystallised grains from the deformed (unrecrystallised) ones in case of sub-micron grain-sized materials characterized by FEG SEM [17]. Figure 5 shows the recrystallised grains in the GOS map where the recrystallised grains with GOS ≤1 are coloured blue in the sample annealed at 300 °C for 1 h. These grains have low angle misorientations ($2 \leq \theta \leq 5$) and are few in number or are completely absent within the grains.

Microhardness measurements

Figure 6a presents the variation of Vickers microhardness after 1 h annealing at different temperatures. The average hardness decreased gradually from ~2 GPa (as-ECAPed) to ~1.7 GPa after annealing at 150 °C. There was an increase in the scatter at 250 °C compared with 150 °C. The hardness continuously decreased almost linearly with increasing temperature from 250 °C through 400 °C. The region between 150 and 250 °C is the stage of recovery, where the stored energy due to prior cold work is

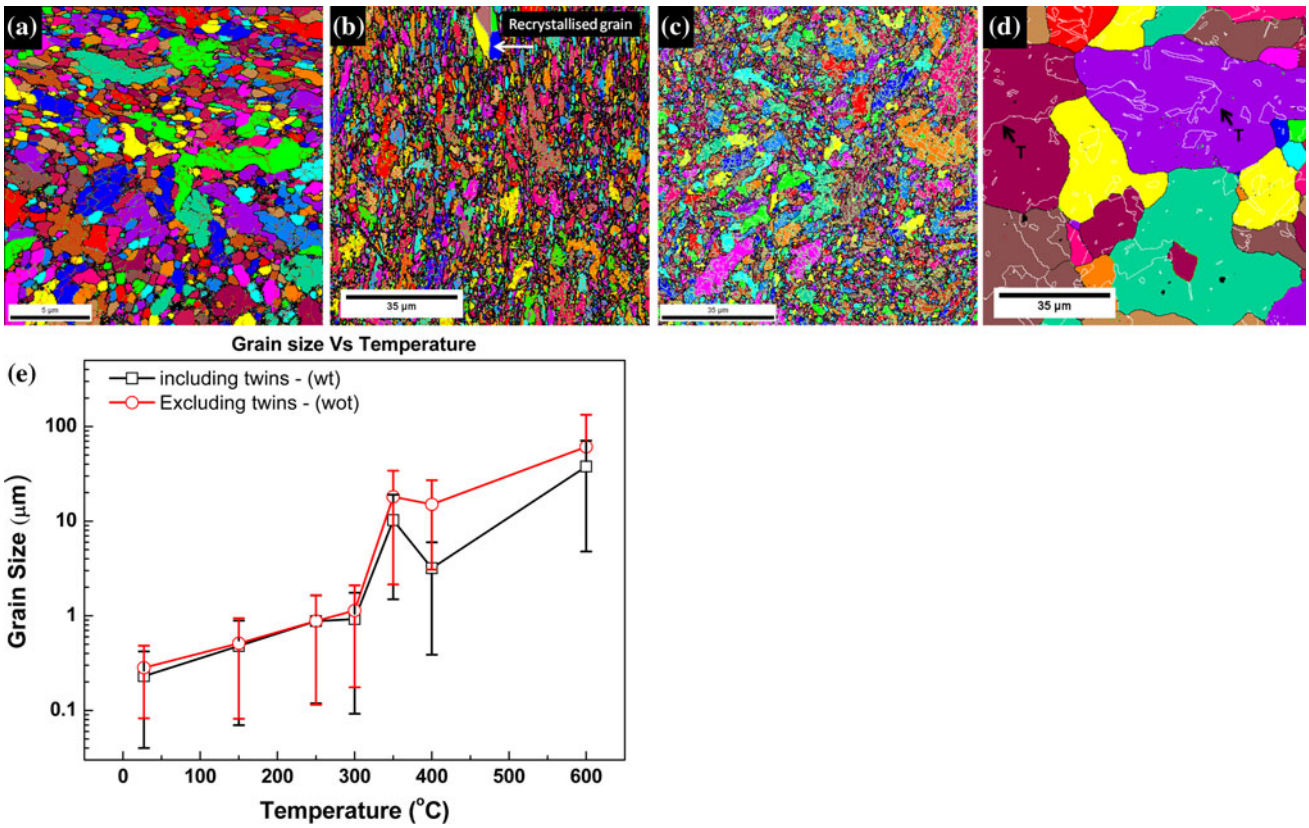

Fig. 3 Microstructures of the as-ECAPed Nickel after 12 passes (**a**), and the annealed samples at 250 °C (**b**), 350 °C (**c**), 400 °C (**d**) and the corresponding grain size plot (**e**). Twins are marked as *T*

recovered. The drop in hardness above 250 °C onwards is due to recrystallisation. Recrystallisation was complete after annealing at 350 °C. This is also clear from Fig. 4b, where the GOS value reaches a minimum at 350 °C for 1 h. The mean GOS and GAM values after annealing at 350 °C is nearly the same (∼0.6°) for an average wot-grain size of ∼18 μm. The values for these two parameters for the sample annealed at 400 °C for 1 h are ∼0.5 and ∼0.7 for an average wot-grain size of ∼15 μm. After annealing at 600 °C for 1 h, there is a slight increase in the GOS value, which is attributed to significant grain coarsening (mean wot-grain size ∼61 μm). (The mean GOS and GAM values are ∼0.7° and ∼ 0.9°, respectively for an average wot-grain size of ∼61 μm.) The increase in the GOS value after 600 °C annealing is due to the drastic increase in the average wot-grain size from 15 to 61 μm. Cho et al. [18] have pointed out that the GOS value is strongly dependent on grain size and this results support this view. Evidently, a large number of measurements in a grain will lead to a statistically increased deviation from the average orientation and hence a higher GOS value.

The changes in the mean grain size with the annealing temperature for 12-pass Nickel are presented in Fig. 6a and the variations in the Vickers microhardness with the annealing temperature for the same material are plotted in Fig. 6b. These hardness values are compared in Fig. 6b with those for 8-pass nickel of different starting grain sizes, the data for which are taken from ref. [11, 19]. However, the comparison is not straightforward because the purity levels of the samples used are not the same- 99.98% in the 12-pass Ni, 99.9% in the study of Neishi et al. [11] and 99.99% in the study of Zhilyaev et al. [19]. It is well-known that recovery/recrystallisation and grain growth are dependent on the impurity level (due to the segregation potential of the impurities to grain boundaries) and the grain size affects the hardness strongly through the Hall–Petch equation. Therefore, this authors merely state that these variations are complex, for which theoretical explanations are yet to be found.

It was shown recently that the H–P relation applies to both microcrystalline and sub-microcrystalline materials, albeit with different slopes for the hardness H_v versus $d^{-0.5}$ plots in the two regions [25]. Figure 7a shows a Hall–Petch (H–P) plot (the H_v versus $d^{-0.5}$ relationship) over the entire range of grain sizes for ECAP 12-pass Ni, annealed at different temperatures for an hour to obtain different grain sizes. This is interesting because by annealing one tends to decrease the dislocation density and increase the grain size,

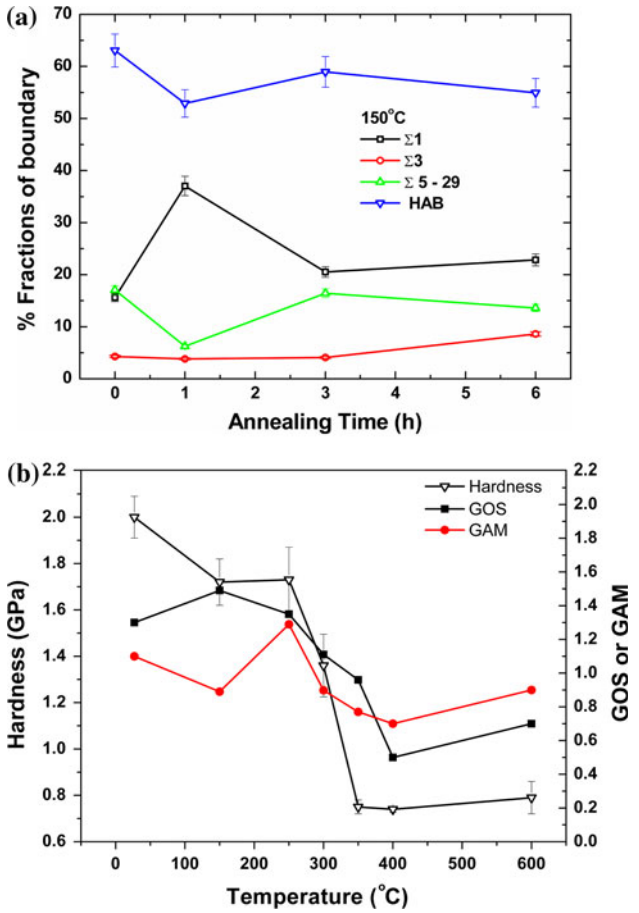

Fig. 4 Boundary fractions as a function of annealing time at 150 °C (**a**) and changes in the GOS and GAM values (**b**) versus annealing temperature

whereas the Hall–Petch relationship has been derived for the situation where the dislocation density increases with increasing grain refinement. Also shown in that figure are the digitized data for pure Ni after 8 ECAP passes, data for which are reported in ref. [11, 19]. In Fig. 7b the H_v versus $d^{-0.5}$ data for 12-pass Ni after all the annealing treatments given in this study are presented, while in Fig. 7c the hardness values of the as-ECAPed 8-pass and 12-pass samples are plotted against the corresponding (wot-grain size)$^{-0.5}$. Evidently, in both these latter plots the H–P relationship is not obeyed. Figure 7d shows the hardness versus (grain size)$^{-m}$ (m = 1,1/3 and ½) plots for this set of measurements and this indicates that a better fit is obtained for m = 1.

Discussion

The AFM phase images in Fig. 2a–c, along with the phase profile plotted in Fig. 2d, indicate a reduction in the local strain in the sample. Careful examination of the phase

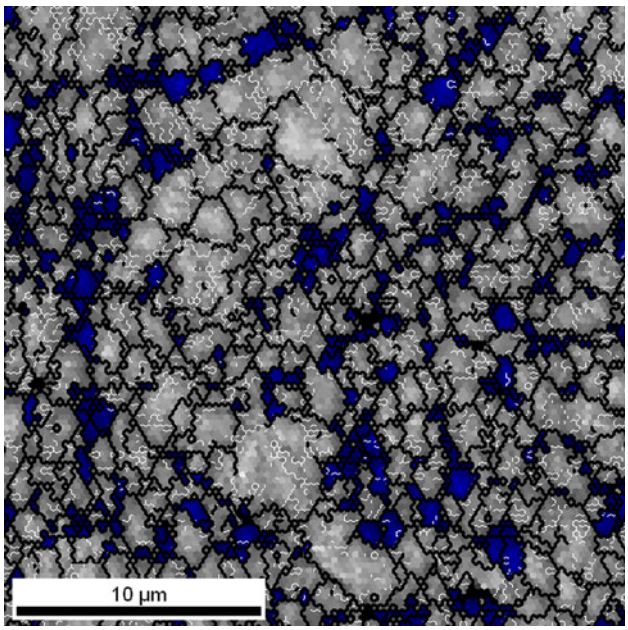

Fig. 5 Microstructure showing the recrystallised grains (coloured *blue*) with GOS ≤1 in the sample annealed at 300 °C for 1 h (Color figure online)

profile shows a gradual increase in the phase shift from the centre of the grain towards the grain boundary, which indicates increased accumulation of defects near the grain boundary. The decrease in the overall phase shift with increasing temperature and time (Fig. 2d), and the gradual increase in the phase shift from the centre to the periphery of the grain are indicative of the greater decrease in the dislocation density (due to annihilation of dislocations) in the interior of the grains compared with the grain boundary regions, both of which are consequences of the recovery of the deformed structure. Also the slope of the phase shift–distance curve from the centre of the grain to its periphery was much smaller than that for the as-ECAPed sample and the sample annealed at 250 °C for 1 h, which indicates a decrease in the density of dislocations on annealing. The average grain size after 12 passes of ECAP obtained from AFM imaging is ~174 nm. After annealing at 250 °C for 1 and 6 h, the grain size increased to ~230 and ~340 nm, respectively. Evidently the IC-AFM technique could be used to identify the grain sizes in the deformed and the recovered microstructures in the sub-micron regime. But, no information regarding the orientation of the crystallites could be obtained. Therefore, it has not been possible to analyse the type of dislocations or the boundary character. A detailed analysis that correlates the changes in the phase image obtained by the AFM technique to the misorientation changes estimated using TEM and EBSD analysis is needed in a future study for obtaining deeper insights.

The average grain size in the as-ECAPed Ni obtained from EBSD and TEM is nearly the same and is equal to

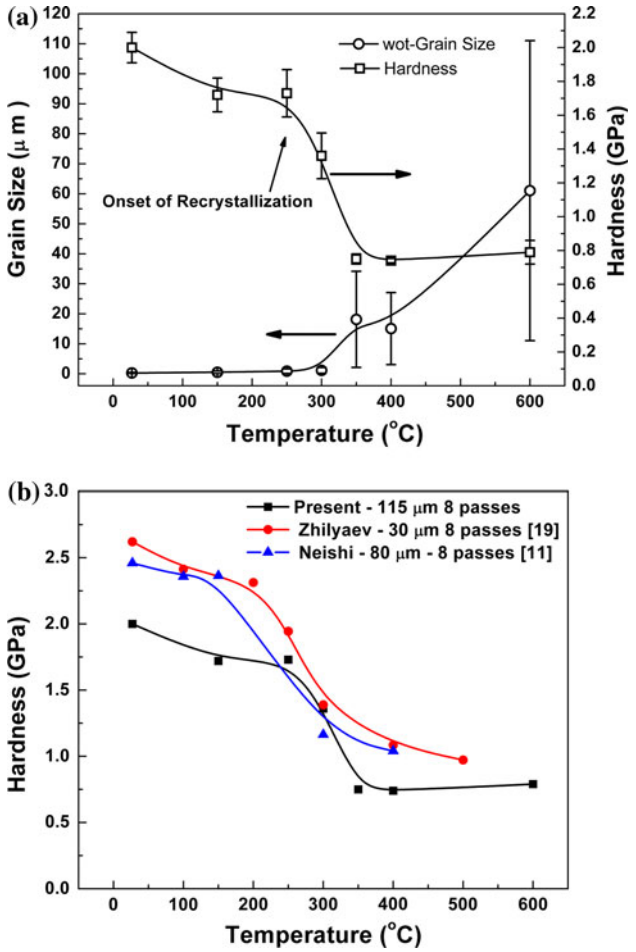

Fig. 6 Change in the wot-grain size versus annealing temperature for a fixed time of 1 h (**a**), and a comparison of the hardness variation in this case with those for ECAPed Ni subjected to 8 passes (**b**)

∼230 nm, and from AFM it is ∼174 nm. In contrast, the grain size obtained from the X-ray diffraction study was significantly lower at ∼70 nm [20]. This difference is because AFM, SEM, EBSD and TEM techniques reveal the average grain size on the surface/a very small and extremely thin sliced section of the sample, while that obtained from X-ray diffraction is representative of the coherently scattering domains, which could be considered as equivalent to the average crystallite size in the bulk [21]. More importantly, the sensitivity of the X-ray method to small-angle grain boundaries and dislocation cell walls is superior to that of the other imaging techniques and therefore in the X-ray method there is a strong possibility of counting the sub-grains and cells also as grains.

The decrease in the average grain size after annealing at 400 °C (Fig. 3d) could be attributed to the nucleation of a large number of fine annealing twins during recrystallisation (as a result of growth accidents during grain boundary migration) [22]. The number fraction of annealing twins is ∼3% for annealing temperatures 250 and 300 °C. In contrast, the number fraction of twins had increased to ∼28 and ∼60%, respectively after annealing at 350 °C and 400 °C for 1 h. The increase in the number fractions of such twins contributes to the observed decrease in the average wt-grain size (Fig. 3e) after annealing at 400 °C for 1 h. (For comparison the wot-grain size is also given in this figure.) A decrease in the twin density (∼41%) after annealing at 600 °C for 1 h could also be deduced from the results of Mahajan et al. and Pande et al. [22, 23] on nickel also, where growth-induced stacking faults were eliminated at the higher temperatures.

Pure Ni after 12 passes of ECAP using the route B_C resulted in a finer grain size (∼230 ± 37 nm) compared with the grain size (∼270 nm) after 8 passes of ECAP [24]. In addition, the fraction of the HABs had increased (from ∼60 to 63.07%) and that of the LABs ($\sum$1) had decreased (from 23.2 to 15.6%) with an increase in the number of passes from 8 [26] to 12 [13]. GAM and GOS values (refer also the TSL manual [25]) were used to quantify the changes that occurred during the annealing of the deformed Ni. Initially, in the recovery stage, an increase in the GOS value indicates the migration of HABs and the accommodation of more LABs (increase in $\sum$ 1 boundaries) might have introduced a steeper gradient in orientation within the grains. In addition, the decrease in the GAM value suggests that the accumulated dislocations or distortions near the grain boundary (deduced from the AFM phase profiles in Fig. 2d) are of low misorientations, formed because of the recovery of the cold worked structure. The increase in the fractions of LABs (<5°) (Fig. 4a) over the HABs after annealing at 150 °C for 1 h lowered the value of GAM. However, this does not affect the value of GOS because it mainly depends on the gradient of the orientation in a grain. By considering this difference between GOS and GAM, it could be stated that GOS is the more useful parameter to follow the recrystallisation of a material than GAM. The GOS value was found to be smaller than the GAM value for the completely recrystallised sample and for the one that had undergone grain growth. In contrast, in the deformed and partially recrystallized condition, no such trend could be observed. The smaller GOS value in the recrystallised and grain growth conditions is due to the reduced gradient in the misorientation within the grains.

The hardness of 8-pass nickel was more than that for 12-pass nickel even though a finer grain size was obtained after 12 passes (Fig. 7c). This could be due to significant recovery during the ECAP processing between 8 and 12 passes for which experimental evidence is presented below. This observation is also similar to what was found, for example, by Molodova et al. [26] in copper. It may be noted that the initial grain size in this study was different (110 μm) from the 80 μm in the study of Neishi et al. [11].

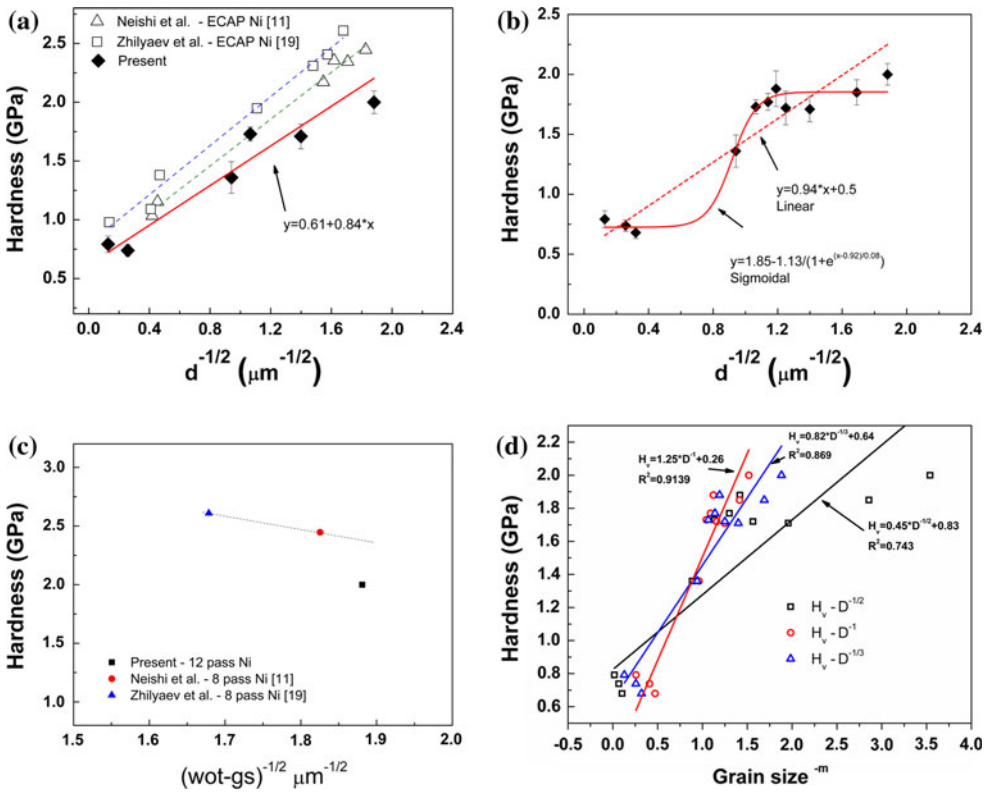

Fig. 7 Hardness—(grain size)$^{-0.5}$ relationship for samples annealed at different temperatures for 1 h (**a**), annealed at different temperatures for different times (**b**), as-ECAPed nickel samples after 8 and 12 passes (**c**), and Hardness—(grain size)$^{-m}$ plots with m = 1, 1/3 and ½ (**d**)

Zhilyaev et al. [19] reported a (mean) hardness of ~2.5GPa after 8 passes for a material with an initial grain size of 30 μm [19]. Interestingly, Zhang et al. [27] found in a nickel sample with an initial grain size of 23 μm that the hardness after 8 and 12 passes are ~3.3 and 4.5 GPa, respectively on the y- plane i.e., the plane defined by the extrusion direction and the transverse direction, of the ECAPed sample. That is, in that experiment, in contrast to this results, the hardness increased when the number of passes was increased from 8 to 12. But, in this study the hardness was measured on the y–z plane i.e., the plane defined by the two directions perpendicular to the extrusion direction. Therefore, this comparison with the earlier study could also mean that grain refinement in orthogonal planes is not similar. There is some experimental evidence available already in this regard [28]. Moreover, when the starting grain size itself is 23 μm as in the study of Zhang et al. [29], the degree of deformation suffered by the individual grains would have been less. It appears, therefore, that the initial hardness, the grain size before ECA pressing, the plane on which the hardness is measured, the amount and nature of impurities present (through their effects on recovery/recrystallisation, grain growth and segregation tendency) and the total degree of strain suffered by the grains/sample all affect the value of the hardness obtained following ECAP. In addition, it was reported in an earlier study [13] that there was an increase in the fractions of special boundaries, which was attributed to an increase in dynamic recovery after 12 passes. In fact, a decrease in the dislocation density (obtained from XRD data) after 12 passes (~1.08×10^{14} m^{-2}) was observed in the present experiments compared with that for 8-pass nickel (~9×10^{14} m^{-2}) [29]. This result supports the idea of an increase in dynamic recovery between the 8th and the 12th pass ECAP operation. This is also seen from the fact that the recrystallisation of 12-pass Ni begins at a slightly higher temperature (250 °C) compared with the 8-pass Ni [11] i.e., the 12-pass ECAP sample has a partially recovered microstructure and therefore recrystallisation commences later than in the case of the 8-pass Ni sample, which had a cold worked structure. These results could also be interpreted to mean that the hardness tends towards a saturation value after going through a maximum. It is noted in this connection that saturation in the hardness value with increasing number of passes has already been reported in oxygen-free Cu [26, 30, 31], pure Al [27, 32, 33], Al alloys [31] and Ni [34]. In Fig. 7c, the hardness values corresponding to two 8-pass Nickel and one 12-pass Nickel as-ECAPed samples are presented in a H–P plot. Consistent with the arguments presented above, Fig. 7c reveals that significant recovery is present between the 8th and the 12th pass (see above) and this has decreased the hardness of the specimen subjected to 12 passes considerably. The path the hardness—(grain size)$^{-0.5}$ relationship should

have followed in the absence of dynamic recovery is shown in this plot by a dotted line. It is clear from Fig. 7a that in this results corresponding to 12-pass ECAP specimens, all annealed for 1 h at different temperatures, and the earlier results pertaining to 8-pass Nickel the H–P relationship is obeyed. However, it should be noted further that for this results, although a mean straight line could be drawn with a decent degree of fit, it was clear that the deviation of some of the datum points from the mean straight line was more significant than in the earlier studies. In the author's opinion, this is due to the onset of the additional dynamic recovery mechanism discussed earlier. But when the data corresponding to all the annealed specimens of this study (produced at different temperatures employing different times) are plotted on a single graph, one obtains a sigmoidal relationship for which there is no theoretical explanation. This is because when one changes the grain size by an annealing process, one alters significantly the internal microstructure of the material, in particular, the dislocation density. Then, the H–P equation will not be valid. As this point has already been discussed in detail by Koch and Narayan [3], there is no need for a separate discussion. The hardness versus grain size data is plotted with different grain size exponents ($-m = 1$, 1/3 and 1/2). The better fit with less deviation from linearity was obtained with $m = 1$. This also suggests that the H–P equation is not obeyed in the case of severely deformed 12 pass ECAP nickel but the data can be represented best with either a sigmoidal fit or a modified H–P relation (see above).

Summary and conclusions

Based on studies on the microstructure, thermal stability and hardness of ultra-fine grained (UFG) Ni produced by 12 passes of equal channel angular pressing (ECAP) through the route Bc, the following conclusions are arrived at:

1. A comparison of the microstructure and hardness of 12-pass ECAP UFG Ni samples with those obtained after 8 passes of ECAP revealed a smaller average wot-grain size (230 nm versus 270 nm in 8-pass Ni), significantly lower dislocation density (1.08×10^{14} m^{-2} versus 9×10^{14} m^{-2} in 8-pass Ni) and lower hardness (2 GPa compared with 2.45 GPa for 8-pass Ni).
2. Study of the thermal stability of the 12-pass UFG Ni revealed that recovery is predominant in the temperature range 150–250 °C and recrystallisation occurred at temperatures >250 °C. The UFG microstructure is relatively stable up to about 400 °C. Due to the lower dislocation density (a partially recovered microstructure) and consequently a lower value of the stored energy, the recrystallisation of 12-pass ECAP Ni occurred at a higher temperature ($\sim$250 °C) compared with the 8-pass Ni ($\sim$200 °C).
3. There is a good correlation between the changes in the grain orientation spread (GOS) and the grain average misorientation (GAM) values with the annealing temperature and the hardness variation with the annealing temperature. When the hardness values were plotted against all the grain sizes obtained in this study by different annealing treatments, the H–P relationship was not obeyed. However, the latter relationship was reasonably well obeyed, if the grain size variation is achieved by varying only the temperatures of annealing, but keeping the time of annealing fixed at 1 h. These results could be understood using the concept of the simultaneous presence of dynamic recovery, a concept for which there is support already in the literature.

Acknowledgements KAP thanks the DFG for a Mercator Visiting Professorship at the Institute of Materials Physics, University of Muenster, Germany. VSS thanks the Indo-US Science and Technology Forum for a sabbatical research fellowship. The authors are grateful to Prof. R.Z. Valiev, Ufa Aviation Technical University, Russia, for supplying the ECAP specimens used in the study. They are also thankful to Dr. Satyam Suwas for his keen interest in this work. KSR thanks A. Sankaran for a discussion on twinning. The facilities provided by the School of Physics and the Centre for Nanotechnology, University of Hyderabad are acknowledged. The EBSD studies were carried out using the SEM facility at the Institute Nano-Science Initiative, Indian Institute of Science, Bangalore and Indian Institute of Technology, Madras, set up with a DST-FIST grant. GW thanks the DFG for support. The authors are thankful to Dr. R. Sundaresan, ARCI, Hyderabad for allowing the use of an annealing furnace.

References

1. Valiev RZ, Islamgaliev RK, Alexandrov IV (2000) Bulk nanostructured materials from severe plastic deformation. Prog Mater Sci 45(2):103
2. Valiev RZ, Langdon TG (2006) Principles of equal-channel angular pressing as a processing tool for grain refinement. Prog Mater Sci 51(7):881
3. Koch CC, Narayan J (2001) The inverse hall-petch effect—fact or artifact? In: Farkas D, Kung H, Mayo M, Swygenhoven H, Weertman J (eds) Materials research Society Symposium. Structure and mechanical properties of nanophase materials—theory and computer simulation versus experiment, Boston, MA
4. Lee TR, Chang CP, Kao PW (2005) The tensile behavior and deformation microstructure of cryo-rolled and annealed pure nickel. Mater Sci Eng A 408(1–2):131
5. Saito Y, Utsunomiya H, Tsuji N, Sakai T (1999) Novel ultra-high straining process for bulk materials–development of the accumulative roll-bonding (arb) process. Acta Mater 47(2):579
6. Tsuji N, Ito Y, Saito Y, Minamino Y (2002) Strength and ductility of ultrafine grained aluminum and iron produced by arb and annealing. Scripta Mater 47(12):893

7. Krasilnikov N, Lojkowski W, Pakiela Z, Valiev R (2005) Tensile strength and ductility of ultra-fine-grained nickel processed by severe plastic deformation. Mater Sci Eng A 397(1–2):330
8. Zhilyaev AP, Gimazov AA, Soshnikova EP, Révész A, Langdon TG (2008) Microstructural characteristics of nickel processed to ultrahigh strains by high-pressure torsion. Mater Sci Eng A 489(1–2):207
9. Valiev RZ, Zehetbauer MJ, Estrin Y, Happel HW, Ivanisenko Y, Hahn H, Wilde G, Roven HJ, Sauvage X, Langdon TG (2007) The innovation potential of bulk nanostructured materials. Adv Eng Mater 9(7):527
10. Dinda GP, Rösner H, Wilde G (2005) Synthesis of bulk nanostructured ni, ti and zr by repeated cold-rolling. Scripta Mater 52(7):577
11. Neishi K, Horita Z, Langdon TG (2002) Grain refinement of pure nickel using equal-channel angular pressing. Mater Sci Eng A 325(1–2):54
12. Zhilyaev AP, Kim BK, Szpunar JA, Baró MD, Langdon TG (2005) The microstructural characteristics of ultrafine-grained nickel. Mater Sci Eng A 391(1–2):377
13. Raju KS, Krishna MG, Padmanabhan KA, Muraleedharan K, Gurao NP, Wilde G (2008) Grain size and grain boundary character distribution in ultra-fine grained (ecap) nickel. Mater Sci Eng A 491(1–2):1
14. Gao N (2008) Applications of differential scanning calorimetry on materials subjected by severe plastic deformation. Mater Sci Forum 584–586 PART 1:255–260
15. Ehrenfest P (1933) Phasenumwandlungen im ueblichen und erweiterten sinn, classifiziert nach den entsprechenden singularitaeten des thermodynamischen potentiales/p. Ehrenfest. In: Proceedings Koninklijke Akademie van Wetenschappen te Amsterdam, N. Z. Voorburgwal (N. V. Noord-Hollandsche Uitgevers Maatschappij), Amsterdam, p 68
16. Humphreys FJ, Hatherly M (2004) Recrystallization and related annealing phenomena. Elsevier, Kiddington Oxford
17. Field DP, Bradford LT, Nowell MM, Lillo TM (2007) The role of annealing twins during recrystallization of cu. Acta Mater 55(12):4233
18. Cho JH, Cho JS, Moon JT, Lee J, Cho YH, Kim YW, Rollett AD, Oh KH (2003) Recrystallization and grain growth of cold-drawn gold bonding wire. Metal Mater Trans A 34 A(5):1113
19. Zhilyaev AP, Nurislamova GV, Baró MD, Valiev RZ, Langdon TG (2002) Thermal stability and microstructural evolution in ultrafine-grained nickel after equal-channel angular pressing (ecap). Metal Mater Trans A 33(6):1865
20. Raju KS, Krishna MG, Padmanabhan KA, Wilde G (2007) On the recovery of the microstructure of heavily deformed nickel produced by ecap. In: Mittemeijer PDIEJ, Leineweber DA, Welzel DU (eds) 5th Size-Strain conference 'Diffraction Analysis of the Microstructure of Materials' (SS-V), Garmisch-Partenkirchen, p 84
21. Warren BE (1990) X-ray diffraction. Wesley series in metallurgy and materials. Addison-Wesley, Addison
22. Mahajan S, Pande CS, Imam MA, Rath BB (1997) Formation of annealing twins in f. c. c. crystals. Acta Mater 45(6):2633
23. Pande C, Imam M, Rath B (1990) Study of annealing twins in fcc metals and alloys. Metal Mater Trans A 21(11):2891
24. Zhilyaev AP, Kim BK, Nurislamova GV, Baró MD, Szpunar JA, Langdon TG (2002) Orientation imaging microscopy of ultrafine-grained nickel. Scripta Mater 46(8):575
25. Tsl oim analysis 5.1 users manual (2008) EDAX are part of AMETEK, Inc., Process and analytical instruments division. http://coen.boisestate.edu/frary/ebsd/OIMAnalysisManual.pdf
26. Molodova X, Gottstein G, Winning M, Hellmig RJ (2007) Thermal stability of ecap processed pure copper. Mater Sci Eng A 460–461:204
27. Zhang Y, Liu JQ, Wang JT, Wu ZB, Liu F Influence of stacking fault energy on microstructures and mechanical properties of fee pure metals by equal channel angular pressing. In: TMS 2010–139th Annual Meeting and Exhibition, Seattle, WA, 2010. TMS 2010–139th Annual Meeting and Exhibition. p 803
28. Prell M, Xu C, Langdon TG (2008) The evolution of homogeneity on longitudinal sections during processing by ecap. Mater Sci Eng A 480(1–2):449
29. Zhilyaev AP, Gubicza J, Nurislamova G, Révész Á, Suriñach S, Baró MD, Ungár T (2003) Microstructural characterization of ultrafine-grained nickel. Physi Solid Appl Res 198(2):263
30. Han S, Lim C, Kim C, Kim S (2005) The microstructural evolution during the equal channel angular pressing process and its relationship with the tensile behavior of oxygen-free copper. Metal Mater Trans A 36(2):467
31. Ferrasse S, Hartwig K, Goforth R, Segal V (1997) Microstructure and properties of copper and aluminum alloy 3003 heavily worked by equal channel angular extrusion. Metal Mater Trans A 28(4):1047
32. Chakkingal U, Suriadi AB, Thomson PF (1998) Microstructure development during equal channel angular drawing of al at room temperature. Scripta Mater 39(6):677
33. Iwahashi Y, Horita Z, Nemoto M, Langdon TG (1997) An investigation of microstructural evolution during equal-channel angular pressing. Acta Mater 45(11):4733
34. Segal VM (1993) Simple shear as a metalworking process for advanced maerials technology. In: First International conference on Processing Materials for Properties, Honolulu, p 947